

Research of radon diffusion behavior in liquid scintillator

Zhongfang Xu^a, Cong Guo^{b,c,d}, Jincang Liu^{b,c,d}, Yongpeng Zhang^{*b,c,d}, Peng Zhang^{b,c,d},
Changgen Yang^{b,c,d}, Quan Tang^{†a}, Yu Liu^a, Chi Li^a, and Tianyu Guan^a

^a*School of Nuclear Science and Technology, University of South China, Hengyang, China*

^b*Experimental Physics Division, Institute of High Energy Physics, Chinese Academy of Sciences, Beijing, China*

^c*School of Physics, University of Chinese Academy of Sciences, Beijing, China*

^d*State Key Laboratory of Particle Detection and Electronics, Beijing, China*

January 18, 2023

Abstract

The background caused by radon and its daughters is an important background in the low background liquid scintillator (LS) detectors. The study of the diffusion behaviour of radon in the LS contributes to the analysis of the related background caused by radon. Methodologies and devices for measuring the diffusion coefficient and solubility of radon in materials are developed and described. The radon diffusion coefficient of the LS was measured for the first time and in addition the solubility coefficient was also obtained. In addition, the radon diffusion coefficient of the polyolefine film which is consistent with data in the literature was measured to verify the reliability of the diffusion device.

Keywords Liquid scintillator · Radon · Diffusion · Solubility

1 Introduction

In order to find rare physical events interested, the sensitive volume of the detector is gradually increased, and the background requirement of the detector is also more strictly in the field of particle physics experiments. Liquid scintillator (LS) is widely used as targets in the large detectors with excellent performance, such as JUNO [1], Borexino [2], KamLand [3]. In order to meet the needs of physical experiments, it is necessary to reduce the background of LS and strictly control source of background.

*ypzhang1991@ihep.ac.cn

†tangquan528@sina.com

Natural radioactive radon dissolved in LS and its natural radioactive daughters, especially lead nuclide with a half-life of 22.3 years, will be the most important background which decides whether the experiment is successful or not. Radon which are from sources, such as air leakage, cover gas and radon emanation for material in contact with LS, can diffuse into LS. The distribution of radon caused by the radon migration properties including the diffusion and solubility in LS need to be studied for providing a reliable basis for future experimental analysis of background caused by radon and lead. The radon isotopes that have an impact on the background are mainly ^{222}Rn and ^{220}Rn . Although they have different decay lifetime and daughters, their diffusion properties should be the same. There is no measurement result of radon diffusion coefficient of LS in the existing literature.

There are generally steady-state method and unsteady-state method for measuring radon diffusion coefficient of other materials [4]. In this paper, the unsteady-state method will be used to measure the radon diffusion coefficient of LS. Compared with the steady-state method, the former has a shorter measurement time (less than one day), while the latter usually has a measurement period of 2 to 4 weeks. Shorter measurement duration can not only improve the measurement efficiency, but also help the stability of measurement and keep the initial state of the measured sample (such as sample volatilization), thus improving the measurement accuracy. However, this requires high sensitivity of radon detector, because it is necessary to monitor the continuously changing radon concentration. In the existing literature, most of the scintillation methods such as $\text{ZnS}(\text{Ag})$ are used to measure radon concentration, which requires a period of time (about 3 hours) for ^{222}Rn and its progenies (^{218}Po , ^{214}Po) to balance. In this paper, SIN-Pin detector is used for the first time to measure concentration of radon diffusion, which can directly measure the generation decay daughter ^{218}Po of ^{222}Rn , thus improving the sensitivity to radon concentration change.

2 Measurement principle

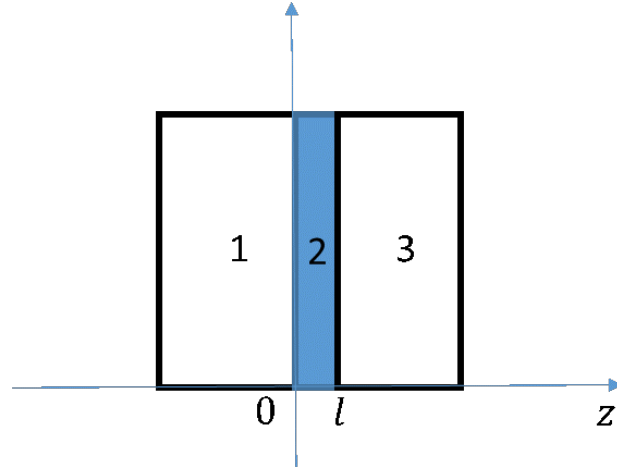


Figure 1: Schematic diagram of diffusion coefficient measurement principle.

Generally, the device for measuring the diffusion coefficient of ^{222}Rn in a certain material can

be simplified as shown in Fig.1, where 2 is the measured material, 1 is the ^{222}Rn source chamber containing a constant ^{222}Rn concentration, and 3 is the collection chamber. When the measured material with thickness l is in contact with the gas with constant ^{222}Rn concentration, ^{222}Rn will first dissolve into the material surface. Because there is a ^{222}Rn concentration gradient in the material, ^{222}Rn will diffuse and decay in the material, and the ^{222}Rn concentration at a certain point in the material will change with position and time. This process is usually called unstable diffusion. After a long time of diffusion and decay equilibrium, the concentration at each point does not change, and the whole system is in a stable diffusion process. The concentration in chamber 1 is C_0 , the concentration in chamber 3 is C_1 . The unstable diffusion process of ^{222}Rn in the material can be described by Fick's second law:

$$\frac{\partial C(z,t)}{\partial t} = D \frac{\partial^2 C(z,t)}{\partial z^2} - \lambda C(z,t) \quad (1)$$

where $C(z,t)$ is the ^{222}Rn concentration at a certain point in the material, D is the diffusion coefficient of ^{222}Rn in the measured material, λ is the decay constant of ^{222}Rn . The number $y(t)$ of ^{222}Rn atoms in the chamber 3 can be solved by Eq.(1)[5]:

$$y(t) = \frac{ADSC_0}{H\lambda} [1 - e^{-\lambda t} + 2 \sum_{n=1}^{\infty} (-1)^n \times \frac{\lambda}{\beta} (1 - e^{-\beta t})] \quad (2)$$

where $\beta = (Dn^2\pi^2/H^2) + \lambda$. S is the ^{222}Rn solubility coefficient for the measured material, A is the measured material surface area (through which Rn diffuses), and H is its thickness.

After ^{222}Rn and its decay daughters reach equilibrium, their activities are almost equal, among which ^{218}Po is the first generation decay daughter, which requires less equilibrium time, so the error of calculating the concentration of ^{222}Rn with the counting rate of ^{218}Po will be smaller. Under the condition that the radon detector keeps the same counting efficiency and detection volume, the ^{222}Rn source and the ^{222}Rn diffused from LS are measured respectively, and the ratio of the counting rates obtained is:

$$\frac{n_2}{n_1}(t) = \frac{\eta\lambda' y_2(t)}{\eta\lambda' y_1(t)} = \frac{\eta\lambda y(t)}{\eta\lambda C_0 V_d} = \frac{y(t)}{C_0 V_d} \quad (3)$$

where n_1 is the count rate of the detector measuring the constant Rn concentration C_0 ; n_2 is the count rate corresponding to the amount of Rn diffused through the measured material; η is the counting efficiency of the Rn detector; λ' is the decay constant of ^{218}Po ; $y_1(t)$ and $y_2(t)$ are the number of ^{218}Po atoms in Rn detector when measuring n_1 and n_2 , respectively; V_d is the volume of Rn detector.

It can be obtained from Eq.(1) and Eq.(2):

$$\frac{n_2}{n_1}(t) = \frac{ADS}{H\lambda V_d} [1 - e^{-\lambda t} + 2 \sum_{n=1}^{\infty} (-1)^n \times \frac{\lambda}{\beta} (1 - e^{-\beta t})] \quad (4)$$

According to Eq. 4, the least-square method is used to fit the ratio n_2/n_1 curve of time function, and the expected values of these two parameters are obtained.

3 Experimental apparatus

3.1 Radon diffusion apparatus

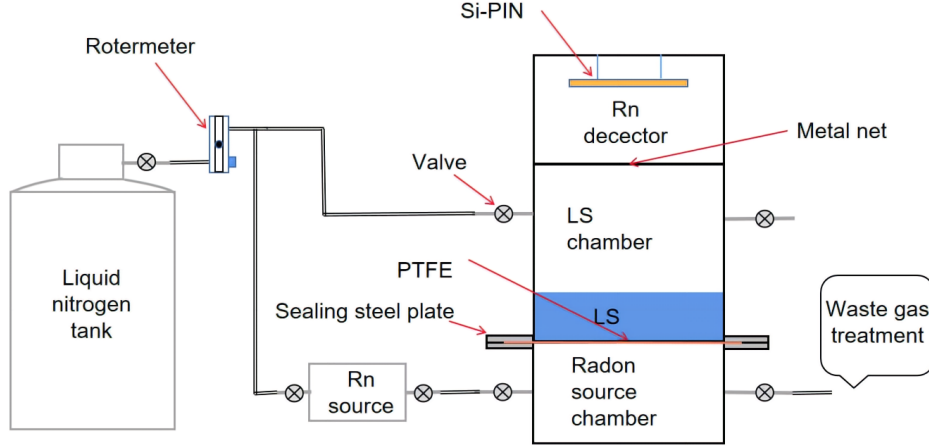


Figure 2: The schematic diagram of the apparatus for the measurement of diffusion and solubility coefficient in LS.

The schematic diagram of the radon diffusion apparatus is shown in Fig.2. The apparatus mainly consists of radon source chamber, LS chamber, Rn detector and some auxiliary devices including liquid nitrogen tanks, radon sources, flow meters, etc. The radon source chamber, LS chamber and the radon detector are made of stainless steel, and the inner diameter is 5 cm, in which the radon source chamber is 6.2 cm high and the LS chamber is 9 cm high, the radon detector is 4.4 cm high. The radon source and LS chamber are sealed by three concentric nylon rubber ring placed on the sealing steel plate to prevent leakage.

The Oleophobic PTFE Membrane is sandwiched in the middle and fixed by screws. The membrane has a gap of 5 μm , which ensures that gas can pass through and LS will not leak from the membrane. The Rn source is a flowing radon source made of $\text{BaRa}(\text{CO}_2)_3$ powder from the Radon Laboratory of South China University [6]. The concentration of ^{222}Rn source can be controlled by adjusting the gas flow rate. The liquid nitrogen tank provides vaporized nitrogen and can keep the outlet pressure stable. The rotameter controls the gas flow rate to be constant, so that the radon source chamber maintains a constant ^{222}Rn concentration.

LS with different thickness can be placed above the membrane. The radon detector is connected to LS chamber through high vacuum cock valve. During the measurement, the two chambers have the same ^{222}Rn concentration (assuming that ^{222}Rn is evenly distributed in the chamber). Since about 90% of the ^{222}Rn daughters are positive [7], and Si-PIN has a negative bias when working [8], which forms an electrostatic field in Rn detector to improve the detection efficiency of ^{218}Po and ^{214}Po . The metal net has the function of electrostatic shielding, which can prevent radon daughters

outside the Rn detector from being collected by electrostatic field, ensuring that the detection range of the Rn detector is above the metal net, and the volume of the detector is 60 cm^3 .

Before the experiment, use vaporized nitrogen to blow the radon detector, and empty the air in the measurement chamber and LS chamber to eliminate the interference of ^{222}Rn in the air.

3.2 Performance of detector

As shown in Fig.3 (a), from the amplitude distribution spectrum (Fig.3(b)) of the pulse signal, the total count of ^{218}Po or ^{214}Po can be counted. For more details of signal output circuit design of Si-PIN detector, please refer to the work of Y.P.Zhang et al.[9].

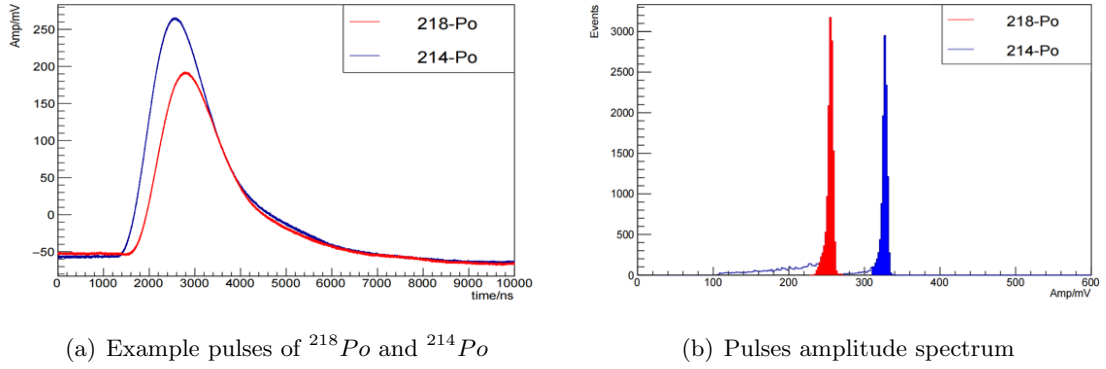


Figure 3: Example pulses of ^{218}Po and ^{214}Po show in (a) and pulses amplitude distributions of ^{222}Rn show in (b).

The comparison of count rates in the Fig.4 shows that diffusion equilibrium has been reached after 50 minutes. In order to reduce the influence of the membrane in the measurement of radon diffusion coefficients in the LS, the data obtained after 50 minutes was used to be analysed.

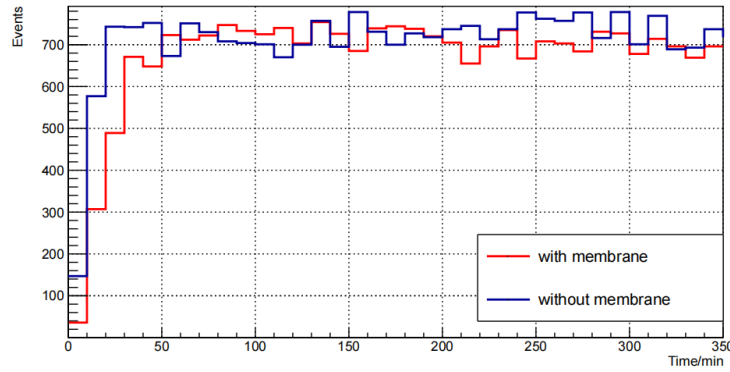


Figure 4: The dependence of the count rate on time for the 0.5 L/min ^{222}Rn source and the count rates with and without the film.

4 Results and discussions

4.1 Results analysis

In this chapter, the diffusion device (Fig.2) described in Section 3 is used to measure the diffusion and dissolution constants of ^{222}Rn in LS, and the results were obtained.

First, we need to measure the count rate of ^{222}Rn source. No LS is added in the LS chamber, and the flow rate of vaporized nitrogen is 0.5L/min. The relationship between the count rate n_1 obtained by radon detector and time is shown in Fig.4.

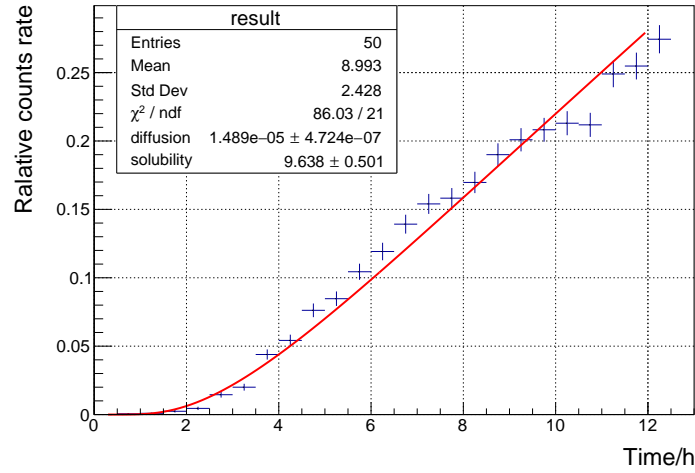


Figure 5: The dependence of the relative count rate on time for the 1 cm LS. The red line is obtained by fitting the experimental data with the equation, the diffusion and solubility are the expected values obtained.

Then, under the same experimental conditions (temperature of $(26 \pm 1)^\circ\text{C}$ and under dry nitrogen atmosphere), adding (0.7 ± 0.05) cm thick LS into the LS chamber (the accuracy of the measuring cylinder is 1 ml by measuring the LS volume), the evaporated nitrogen still flows out at a flow rate of 0.5 L/min. The radon detector measured the count rate n_2 of ^{222}Rn diffusing into the radon detector. Fig.5 describes the measured ratio of n_2/n_1 versus time, and gives the theoretical curve fitted to the experimental data and the values of obtained D and S coefficients. Using the above method, The ^{222}Rn diffusion coefficient and solubility of LS with different thicknesses were measured, as shown in Table 1.

We also can measure the ^{222}Rn diffusion coefficient and solubility of other membranes, just replace this Oleophobic PTFE Membrane with a test membrane. The diffusion coefficient of ^{222}Rn in polyethylene film (PE) has been measured, and compared the results with those of other literatures.

Material	Thickness	Measured data		Literature data
		Diffusion[cm^2/s]	Solubility	Diffusion[cm^2/s]
LS	0.5 cm	$(1.33 \pm 0.10) \times 10^{-5}$	9.34 ± 0.95	-
LS	1 cm	$(1.49 \pm 0.05) \times 10^{-5}$	9.64 ± 0.50	-
PE	0.01 cm	$(2.00 \pm 1.04) \times 10^{-8}$	7.52 ± 3.97	$3.7^{+2.0}_{-1.2} \times 10^{-8}$ [10]

Table 1: Measurement results

4.2 Solubility measurement

According the Eq. 4, the measurement principle can not only obtain the results of the diffusion coefficient but also the solubility. In order to verify the reliability of the results, another method is used to measure the solubility of radon in LS, and a solubility device is designed for this purpose.

At a certain temperature and atmospheric pressure, a gas with a stable concentration of ^{222}Rn is blown into the LS at a certain flow rate. When the ^{222}Rn in the carrier gas reaches the dissolution equilibrium with the LS, the solubility is:

$$S = \frac{C_l}{C_g} \quad (5)$$

Where S is the solubility of ^{222}Rn in LS; C_l is the ^{222}Rn concentration in LS and C_g is the ^{222}Rn concentration in gas.

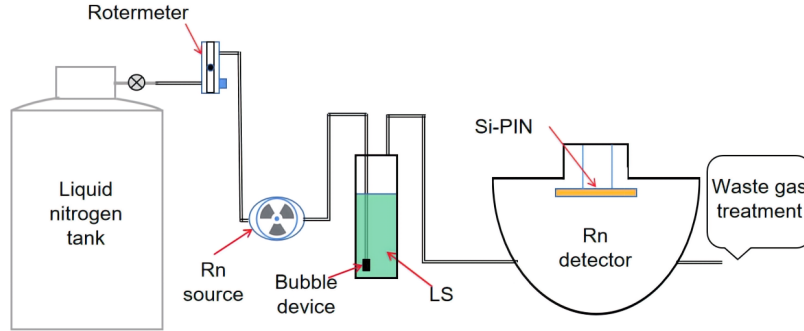


Figure 6: Solubility device.

In most literatures, radon adsorbed in LS is usually measured directly to calculate the solubility of radon in LS. A new method for indirectly measuring the concentration of radon in gas is proposed to measure the solubility. As shown in Fig. 6, the solubility device consists of LS chamber, radon detector and some auxiliary devices. 500ml LS is packed in a stainless steel tank with high sealing property, and the bubble device can improve the efficiency of absorbing ^{222}Rn by LS. Rn detector is a hemispherical detector made of polished stainless steel. Its volume is 1L, and its working principle is the same as that of the radon detector in the previous section.

In order to ensure the tightness of the whole measuring system, knife edge flanges and VCR connectors are used at all connections. The leakage rate of the system is better than 1×10^{-9} Pa·m³/s, which is measured by a helium leak detector (ZQJ-3000, KYKY Technology Co. Ltd).

The ^{222}Rn source (1600 ± 100 Bq/m³) gas is introduced into the LS at a flow rate of 0.5 L/min, and the Rn detector continuously monitors the gas coming out of the LS. The obtained count rate changes with time as shown in fig7. The counting rate continued to rise in the first 40 minutes, and then stabilized in a certain range. It can be concluded that ^{222}Rn has reached the solubility equilibrium in LS at 40 minutes.

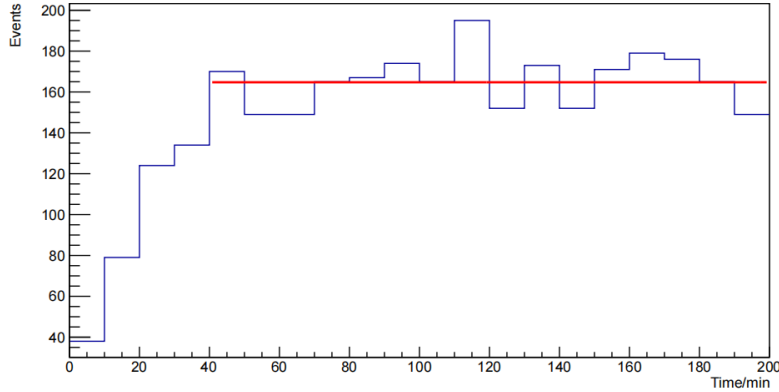


Figure 7: Count rate of ^{222}Rn source gas passing through LS at a flow rate of 0.5 L/min changes with time, the red line is the expected value of ^{222}Rn source count.

According to Eq.(5), the solubility of ^{222}Rn in LS is obtained from Eq.(6):

$$S = \frac{\Delta n V_g}{n_1 V_l} \quad (6)$$

Where Δn is the difference of the first 40 minutes count between ^{222}Rn source after LS absorption and ^{222}Rn source. n_1 is the average count rate of ^{222}Rn source every 40 minutes. V_g is the volume of ^{222}Rn source flowing into LS within 40 minutes, and V_l is the volume of LS. Compared with the air, the concentration of ^{222}Rn source is much higher, so the background of ^{222}Rn in LS can be ignored. The temperature in the experiment is stable at $(27 \pm 1)^\circ\text{C}$. By substituting the measured data into the formula, we can get $S = (9.6 \pm 2.1)$.

5 Conclusion

By understanding the distribution of radon due to diffusion in the LS, the effect of radon on the background in low background LS detectors can be further analysed. A dedicated device for measuring diffusion coefficients and solubility coefficients has been developed. The radon diffusion coefficient in the LS was measured for the first time and it was $(1.49 \pm 0.05) \times 10^{-5} \text{ cm}^2/\text{s}$. Moreover, the radon solubility is 9.64 ± 0.50 .

To ensure the reliability of the diffusion measurement results, two approaches were taken to verify this. One is to use this device to measure the radon diffusion coefficient of PE films and the results indicate good agreement with the literature data. The second is to adopt a new method of indirectly measuring the radon solubility by installing another device dedicated to the measurement of radon solubility coefficient in the LS. The experimental results show that the solubility results of the two devices are self-consistent.

The developed devices can also be used to measure ^{222}Rn diffusion coefficient and solubility coefficient in various materials.

6 Acknowledgements

This work is supported by the National Natural Science Foundation of China (Grant No. 11875280, No.11905241), the Innovative Project of the Institute of High Energy Physics (Grant No. Y954514), and the National Natural Science Foundation of China - Yalong River Hydropower Development Co., LTD. Yalong River Joint Fund (Grant No. U1865208).

References

- [1] Fengpeng An et al. Neutrino Physics with JUNO. *J. Phys. G*, 43(3):030401, 2016.
- [2] G. Alimonti et al. The borexino detector at the laboratori nazionali del gran sasso. *Nucl. Instr. and Meth. A*, 600(3):568–593, 2009.
- [3] K. Eguchi et al. First results from KamLAND: Evidence for reactor anti-neutrino disappearance. *Phys. Rev. Lett.*, 90:021802, 2003.
- [4] Andrey Tsapalov, Loren Gulabyants, Mihail Livshits, and Konstantin Kovler. New method and installation for rapid determination of radon diffusion coefficient in various materials. *Journal of Environmental Radioactivity*, 130:7–14, 2014.
- [5] M. Wojcik, W. Wlazole, G. Zuzel, and G. Heusser. Radon diffusion through polymer membranes used in the solar neutrino experiment Borexino. *Nucl. Instrum. Meth. A*, 449:158–171, 2000.
- [6] L.F. Xie, J.C. Liu, S.K. Qiu, C. Guo, C.G. Yang, Q. Tang, Y.P. Zhang, and P. Zhang. Developing the radium measurement system for the water cherenkov detector of the jiangmen underground neutrino observatory. *Nuclear Inst. and Methods in Physics Research, A*, 976:164266, 2020.
- [7] P. Kortrappa, S.K. Dua, P.C. Gupta, and Y.S. Mayya. Electret - a new tool for measuring concentrations of radon and thoron in air. *Health Phys*, 41:35–46, 1981.
- [8] Y.Y. Chen, Y.P. Zhang, Y. Liu, J.C. Liu, C. Guo, P. Zhang, S.K. Qiu C.G. Yang, and Q. Tang. A study on the radon removal performance of low background activated carbon. *JINST*, 17:P02003, 2022.

- [9] Y.P.Zhang, J.C.Liu, C.Guo, et al. The development of ^{222}Rn detectors for juno prototype. *Radiation Detection Technology and Methods*, 2:5, 2018.
- [10] Wolfgang Rau. Measurement of radon diffusion in polyethylene based on alpha detection. *Nuclear Instruments and Methods in Physics Research A*, 664:65–70, 2012.